Skin Lesion Segmentation Using Attention-Based DenseUNet

Anwar Jimi[1], Hind Abouche[1], Nabila Zrira[2] and Ibtissam Benmiloud[1]
[1]*MECAtronique Team, CPS2E Laboratory National Superior School of Mines Rabat, Morocco*
[2]*ADOS Team, LISTD Laboratory National Superior School of Mines Rabat, Morocco*

Keywords: Skin Lesion Segmentation, DenseNet, Deep Learning, DenseUNet, Attention.

Abstract: Skin lesion segmentation in dermoscopic images is still a challenging problem due to the blurry borders and low contrast of the lesions. Deep learning networks, like U-Net, have been successfully used to segment medical images over the past few years, and their performance has improved in terms of time and accuracy. This paper proposes an automated method for segmenting lesion boundaries that combines two architectures (i.e., the U-Net and the DenseNet as backbone) as well as the attention mechanism. Moreover, we also used adaptive gamma correction to enhance the contrast of the image, which considerably enhanced the segmentation results. Furthermore, we trained our model on the ISIC 2016, the ISIC 2017, and the ISIC 2018 datasets. Finally, the qualitative and quantitative experimental results of the skin lesion segmentation are very promising.

1 INTRODUCTION

Skin cancer is the most prevalent type of cancer worldwide. As ozone levels decrease, the atmosphere increasingly loses its protective filtering function, and the surface of the Earth receives more solar ultraviolet (UV) radiation. According to the World Health Organization (WHO), every 10% reduction in the ozone layer would lead to 4,500 melanoma cases and more than 300,000 non-melanoma instances of skin cancer (Organization et al., 2017). The prevalence of melanoma is increasing globally, but UV radiation is the principal cause of melanoma growth. Melanoma causes more than 20,000 deaths in Europe each year. Currently, 132,000 cases of melanoma and 2 to 3 million cases of non-melanoma skin cancer are reported annually worldwide. According to the Skin Cancer Foundation (SCF), skin cancer accounts for one in three cancer diagnoses and one in five lifetime cases of cancer in the United States (US).

Basal cell carcinoma and squamous cell carcinoma are two types of non-melanoma skin malignancies. Although they are rarely fatal, surgical treatments are often disfiguring and traumatic. It is challenging to identify historical trends in the occurrence of non-melanoma skin cancers since trustworthy registries for these malignancies have not yet been established. Nevertheless, particular research in Australia, Canada, and the US shows that the prevalence of non-melanoma skin cancers more than tripled between the 1960s and 1980s.

The most common type of skin cancer that results in mortality is malignant melanoma, which is also the one that is reported and diagnosed more frequently than non-melanoma skin cancer. The prevalence of malignant melanoma has considerably increased since the early 1970s, by an average of 4% per year in the US. Several studies have shown that the risk of malignant melanoma is related to genetic and personal characteristics, as well as a person's UV radiation behavior. Malignant melanoma is more common in white people with blue eyes and red or blond hair. Australia has the highest incidence, where the annual incidence is more than 10 and 20 times higher than in European women and men, respectively.

Automatic skin lesion segmentation is a critical step in Computer-Aided Diagnosis (CAD). However, because skin lesions vary significantly in shape, size, and color, this task remains difficult. Furthermore, the borders of certain lesions are uneven and hazy. Thus, today, computer vision and image processing approaches are being used to improve dermoscopy in order to develop tools that are capable of correctly diagnosing lesions, with the goal of improving access to reliable data to assist doctors. This enhancement can be implemented in a number of ways, including the detection of lesions, their borders, and colors, as well as the segmentation of different types of lesions.

Deep learning, which is based on Convolutional Neural Networks (CNNs), has recently gained promi-

Jimi, A., Abouche, H., Zrira, N. and Benmiloud, I.
Skin Lesion Segmentation Using Attention-Based DenseUNet.
DOI: 10.5220/0011686400003414
In *Proceedings of the 16th International Joint Conference on Biomedical Engineering Systems and Technologies (BIOSTEC 2023) - Volume 3: BIOINFORMATICS*, pages 91-100
ISBN: 978-989-758-631-6; ISSN: 2184-4305

nence in machine learning and computer vision, particularly in the semantic image segmentation area (Litjens et al., 2017). In this paper, we propose a new automatic approach for the segmentation of skin lesions using attention-based DenseUNet. In addition, we used adaptive gamma correction to enhance the contrast of the image and hence improve the segmentation result.

The following is a summary of this paper. An overview of skin cancer is presented in Section 2. The state-of-the-art of skin lesion segmentation is briefly introduced in Section 3. Section 4 describes the used datasets and our proposed approach. Section 5 illustrates implementation details, segmentation metrics and experimental results. Section 6 is about discussion and future work. Finally, we conclude this paper in Section 7.

2 SKIN CANCER

The most dangerous kind of skin cancer is melanoma (Capdehourat et al., 2011). It spreads easily to any organ and expands swiftly. Skin cells called melanocytes are the source of melanoma. These cells create the dark pigment known as melanin, which gives skin its color. Though it only accounts for around 1% of all skin malignancies, melanoma is the most common death from skin cancer. Early melanomas are often recoverable, so it's crucial to be able to identify them. Melanoma can present as raised bumps, scaly patches, open sores, or moles. Table 1 illustrates the indicators which are offered by the "ABCDE" memory aid from the American Academy of Dermatology (Nachbar et al., 1994) to determine if a lesion on the skin can be melanoma:

Asymmetry: The two halves are not identical;

Border: There are rough edges;

Color: With varying tones of brown, black; gray, red, or white, the color is mottled and irregular;

Diameter: The spot is larger than the eraser's tip (6.0 mm);

Evolving: The spot is either brand-new or is altering in size, shape, or color.

Moreover, Figure 1 shows the comparison between malenoma and non melanoma skin lesion based on the ABCDE rule.

3 RELATED WORK

In this section, we describe and present relevant work performed on the issue of skin lesion segmentation. It focuses on recent approaches that have incorporated deep learning methods for lesion segmentation.

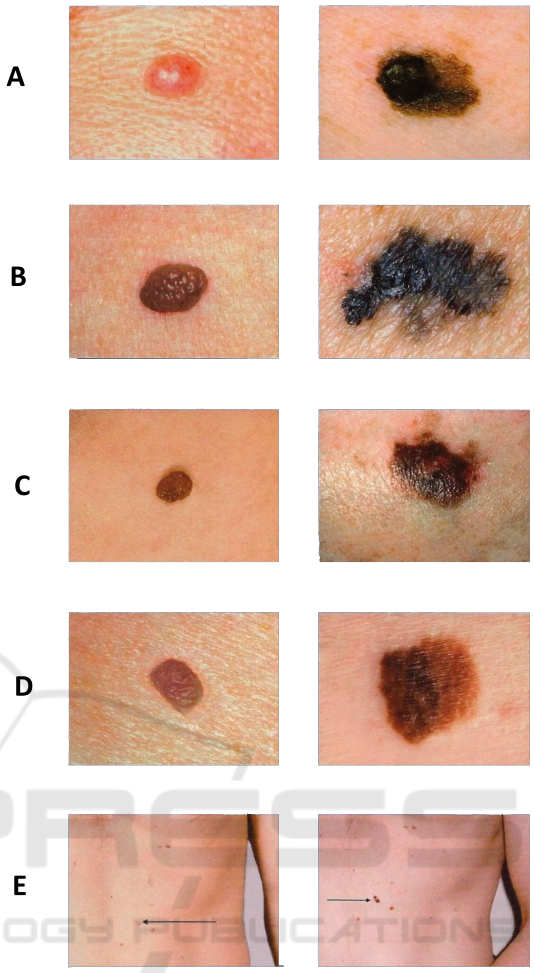

Figure 1: Right: normal lesion. Left: melanoma lesion.

In 2015, Wang et al. presented the U-Net (Ronneberger et al., 2015) network for segmenting medical images. A neural network called U-Net uses symmetric encoders and decoders, a structure that has demonstrated exceptional productivity in the area of medical imaging. Additionally, a variety of enhanced models built on the U-Net framework have been put forth to further increase the accuracy of computer-aided medical imaging diagnostic activities.

Inspired by the U-Net, Sulaiman et al. (Vesal et al., 2018) suggested the SkinNet model based on the CNN. The CNN architecture that has been suggested represents a redesign of the U-Net. SkinNet uses dilated convolutions specifically in the lowest layer of an encoder branch in the U-Net, to provide a more global context to the extracted features from the image. Furthermore, the authors swap out usual convolution layers in both the U-Net encoder and decoder

Table 1: Comparison between melanoma and normal lesion.

Indicator	Melanoma	Normal
Asymetry (A)	Asymmetrical	Symmetrical
Border (B)	Uneven	Even
Color (C)	Multiple colors	One color
Diameter (D)	Larger than $\frac{1}{4}$inch	Smaller than $\frac{1}{4}$inch
Evolving (E)	Changing in size, color, shape	Ordinary mole

parts, using dense convolution blocks, to more effectively combine multi-scale visual information. The ISIC 2017 dataset was used to assess the SkinNet model, which received an IOU score of 76.7% and a dice coefficient of 85.10%. Galdran et al. (Galdran et al., 2017) utilized the U-Net architecture as well as color constancy techniques to maintain the estimated illumination information while normalizing the color over the whole dataset. This makes it possible for normalized images to fluctuate in color and lighting at random while being trained. On the ISIC 2017 dataset, they attained a dice coefficient of 84.60%. Berseth et al. (Berseth, 2017) created a U-Net architecture for segmenting skin lesions based on the probability map of the image dimension, then trained the model using ten-fold cross-validation.

Currently, in deep learning algorithms, certain models are frequently employed as pre-trained encoders. Many pre-trained algorithms like ResNet, EfficientNet, and MobileNet can train the U-Net model with greater accuracy. Kashan et al. (Zafar et al., 2020) presented a system for automatically segmenting lesion borders, that created a new architecture known as Res-Unet by combining the U-Net and ResNet architectures. Additionally, they employed image inpainting to remove the hair, which dramatically enhanced the segmentation outcomes. The model was assessed using the ISIC 2017 and PH2 datasets. On the ISIC 2017 test set, the approach achieved a Jaccard Index of 0.772. Whereas, on the PH2 dataset it achieved a Jaccard Index of 0.854. Baheti et al. (Baheti et al., 2020) introduced a novel architecture called Eff-UNet that integrated the efficiency of compound-scaled EfficientNet as the encoder for feature extraction with the U-Net decoder for recreating the fine-grained segmentation map. Wibowo et al. (Wibowo et al., 2021) suggested a lightweight encoder-decoder built on U-Net and MobileNetV3 to enhance the network architecture's performance. Also, they employed some methods like the filling-in-the-hole post-processing method and stochastic weight averaging learning schema, to enhance the segmentation map during testing. To prevent overfitting, the authors utilized random augmentation by increasing image variety in the training dataset. Zahangir et al. (Alom et al., 2018) proposed a Recurrent Residual Convolutional Neural Network (RRCNN) and a Recurrent Convolutional Neural Network (RCNN) based on the U-Net. Proposed models make use of the capabilities of RCNN, Residual Networks, and U-Net. RCNN and RRCNN both facilitate quick network training and provide excellent feature representation for segmentation tasks.

The Google Deep Mind team made the initial suggestion for the attention mechanism in an image classification challenge, triggering a wave of attention mechanism research (Mnih et al., 2014). Wang et al. (Wang et al., 2018) introduced a non-local block to obtain the reliance of the global information on the pixel-level relationship. Chaitanya et al. (Kaul et al., 2019) suggested a novel technique to incorporate attention within CNN using feature maps produced by a different convolutional auto-encoder. Hu et al. (Hu et al., 2018) affirmed that by explicitly describing the interdependencies between channels, SE-Net adaptively recalibrates channeled feature responses. Woo et al. (Woo et al., 2018) developed Convolutional Block Attention Module (CBAM), a straightforward yet efficient attention module for feed-forward convolutional neural networks, using a feature map in between.

4 MATERIALS AND METHODS

In this section, we firstly introduce the used dermoscopic images of melanocytic lesions. Secondly, we present all the techniques used in the preprocessing step . Thirdly, we describe in detail the model architecture that is used in the context of lesion segmentation. As shown in Figure 2, the approach is divided into three major steps.

4.1 Used Datasets

We evaluated the proposed network on three dermoscopic image datasets, including the ISIC-2016 challenge dataset (Gutman et al., 2016), the ISIC-2017 challenge dataset (Codella et al., 2018) and the ISIC-2018 challenge dataset (Codella et al., 2019; Tschandl et al., 2018). The International Skin Imaging Collab-

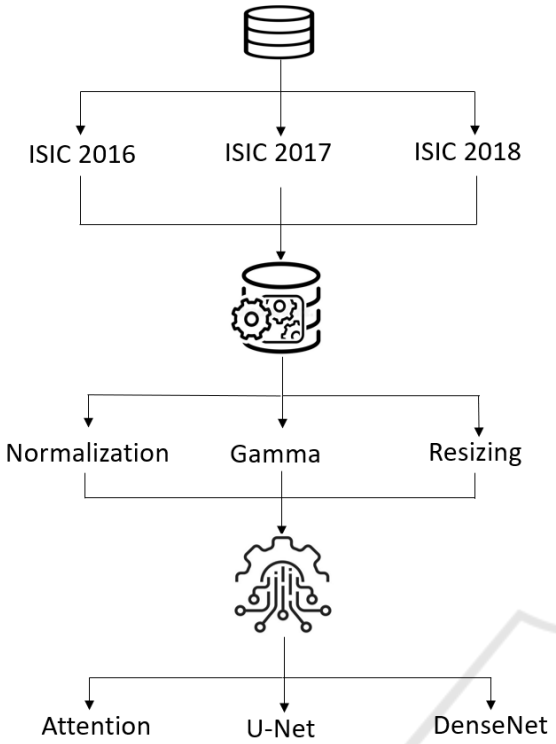

Figure 2: Diagram of the proposed model.

orative (ISIC) offers expertly annotated digital skin lesion image datasets from all over the world to support the computer-aided diagnosis of melanoma and other skin lesions. These images will help to provide an automated and effective computer diagnosis. An overview of the ISIC 2016, ISIC 2017, and ISIC 2018 datasets is shown in Table 2.

There are 900 training images and 379 test images in the ISIC 2016 challenge dataset. The ISIC 2017 skin lesion challenge dataset included 2,000, 150, and 600 images for training, validation, and testing, respectively. The dimensions of the images ranged from 556×679 to 4499×6748 pixels. The ISIC 2018 skin lesion dataset challenge included 2,594 images for training. This dataset was divided into training (1,815), validation (259), and test sets consecutively (not randomly). The image sizes ranged from 556×679 pixels to $4,499 \times 6,748$ pixels. The sample images from the datasets are displayed in Figure 3.

4.2 Image Preprocessing

Deep learning architectures can successfully learn from unprocessed image data. However, on properly preprocessed images, they usually perform better. The preprocessing used in this work is described as follows.

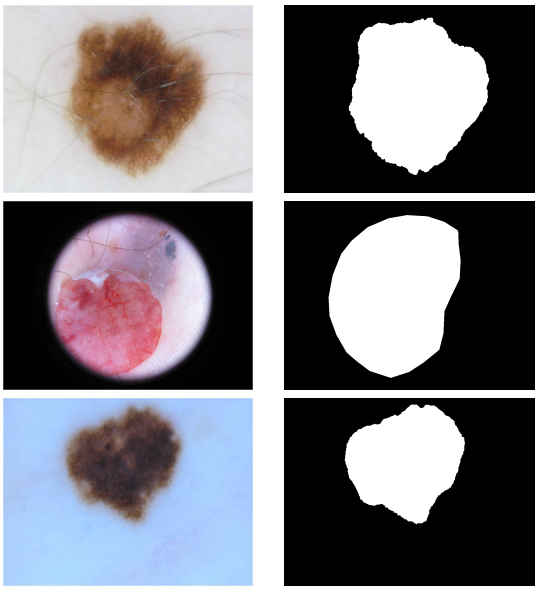

RGB images Ground truths

Figure 3: Examples of skin lesion images from ISIC datasets.

4.2.1 Image Resizing

The images and associated ground truths were scaled to 256×256 pixels ($height \times width$) to adjust for variances in image size within the datasets.

4.2.2 Image Normalization

Each pixel in the images and ground truth masks has 8 bits in size and can have a value between 0 and 255. The input image was divided by 255 to normalize the images, changing each pixel's normal value range from 0 to 1. When the ground truth mask is rounded up or set to the ceiling, it is converted to a binary representation (0 for background and 1 for foreground).

4.2.3 Contrast Enhancement

Contrast enhancement plays an important role in improving visual quality in computer vision, pattern recognition, and image processing.

In this paper, we use adaptive gamma correction with weighting distribution (Huang et al., 2012) to improve the image quality for better segmentation. Three main steps make up the method. The flowchart of the approach is shown in Figure 4.

First, based on probability and statistical inference, the histogram analysis provides the spatial information of a single image. The weighting distribution is employed in the second stage to smooth the fluctuant phenomenon and prevent the creation of unwanted artifacts. Gamma correction can automatically improve the image contrast in the third and final

Table 2: Description of the three datasets.

Dataset	ISIC 2016	ISIC 2017	ISIC 2018
Total number of images	1,279	2,750	2,594
Image size (pixel)	576×768 to $2,848 \times 4,288$	556×679 to $4,499 \times 6,748$	556×679 to $4,499 \times 6,748$

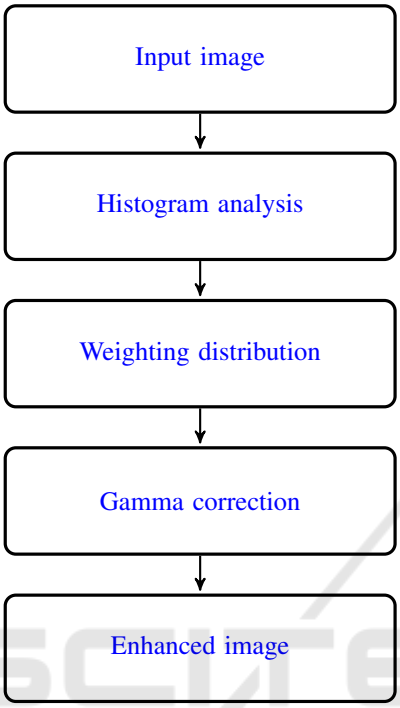

Figure 4: Flowchart of Adaptive Gamma Correction With Weighting Distribution.

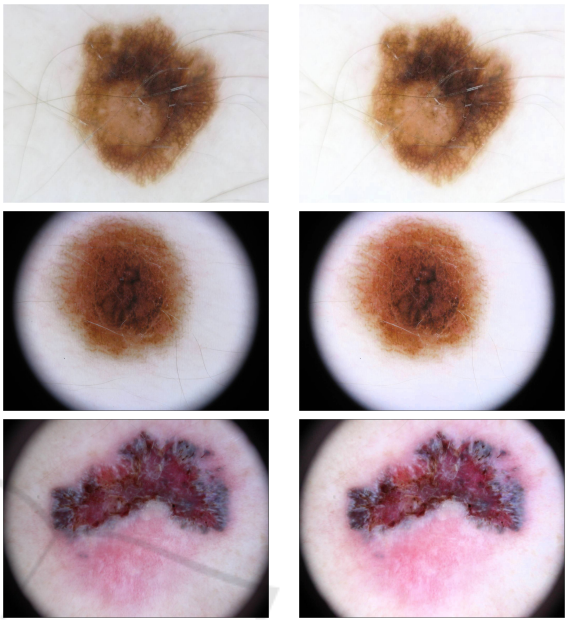

Figure 5: Gamma correction.

step by using a smoothing curve. The results of the image enhancement are shown in Figure 5.

4.3 Model Architecture

Deep learning models are currently being utilized to solve object detection and visual recognition problems. For semantic segmentation, CNN models have demonstrated a significant advantage over semi-automated techniques. The U-Net architecture based on the encoder-decoder approach has achieved great results in the segmentation of medical images.

Common layer combinations make up CNN models (i.e., convolutional layer, max-pooling, batch normalization, and activation layer). In the area of medical diagnostics, CNN architectures have been widely applied.

For this purpose, ISIC datasets are used to train a CNN architecture. The network architecture takes insight from both U-Net and DenseNet as well as the mechanism of the attention gate as shown in Figure 6.

The convolutional side (i.e., contracting path) is based on the DenseNet architecture. The idea of DenseNet was first suggested by Huang et al. (Huang et al., 2017) and leads to significant advancements in state-of-the-art scores compared to earlier models like ResNet (He et al., 2016) and ResNeXt (Xie et al., 2017) in image classification tasks like ImageNet.

DenseNet is made up of a dense block and a transition block as its two main construction blocks. A dense block consists of several normalized 3×3 convolution layers, where the outputs of each layer are concatenated with each of the feature maps entering the succeeding layers to encourage feature reuse. A dense block has n layers and $n!$ skip connections. Each layer produces a feature map with a constant depth of k, causing $n \times k$ channels to leave the dense block. The transition block is made up of a normalized 1×1 convolution to decrease the depth of the feature maps and a 2×2 average pool with stride 2 to halve the resolution.

In the U-Net architecture, Oktay et al. (Oktay et al., 2018) first suggested the Attention Gate (AG). The AG attention module automatically and adaptively learns to concentrate on the various sizes and shapes of the target structures in medical images. The model under the AG strain implicitly learns to emphasize important features useful for a particular task while removing unnecessary regions from an input

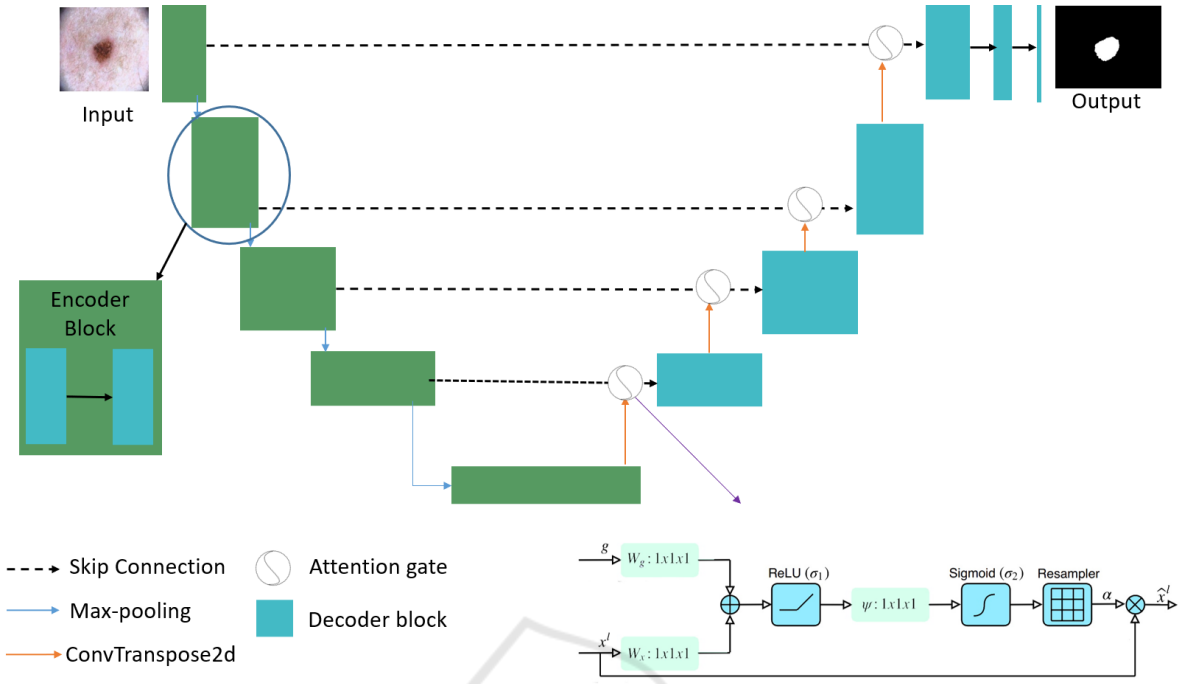

Figure 6: Diagram of the proposed model.

image. Figure 7 shows a schematic of the AG.

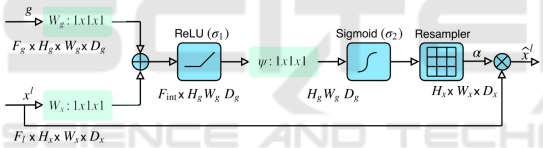

Figure 7: Attention gate (Oktay et al., 2018).

As following is how the attention mechanism functions:

- There are two inputs to the attention gate, vectors x and g.
- g, gating signal comes from the next lowest layer of the network.
- x, comes from skip connections.
- The two vectors are added element by element. This process results in aligned weights getting larger while unaligned weights getting relatively smaller.
- The resulting vector passes through a Rectified Linear Unit (ReLU) activation layer and a 1×1 convolution that reduces the dimensions.
- This vector passes through a sigmoid layer that scales it between [0, 1], generating the attention coefficients (weights), where coefficients nearer 1 indicate more pertinent features.
- The attention coefficients are upsampled to the original dimensions of the x vector using trilinear interpolation. The attention coefficients are multiplied element-wise to the original x vector, this scales the vector based on relevance.

4.4 Network Training

Our model was trained over 100 epochs with early stopping to avoid overfitting. The learning rate is decreased if, after 10 epochs, the model's loss is not reduced. After nearly 40 epochs, our model came to an end. The hyperparameters utilized to train our model are listed in the Table 3.

Table 3: Hyperparameters maintained during training.

Name	Value
Input Size	$256 \times 56 \times 3$
Batch Size	32
Learning Rate	1×10^{-4}
Optimizer	Adam
Epoch	100
Loss Function	Binary Crossentropy

5 EXPERIMENTAL RESULTS

In this section, we first explain the implementation details of our approach, and then we present the results of our model compared to the other state-of-the-art al-

gorithms that utilize the same datasets using segmentation metrics.

5.1 Details of Implementation

We implemented our network using TensorFlow on a GPU T4 and P100 in Google Colab. All training and testing phases were performed in the same environment using Python 3.5 as the programming language and the TensorFlow 2.5.0 framework for deep learning.

5.2 Segmentation Metrics

In order to evaluate semantic segmentation techniques in the literature the following measures have been employed (Pereira et al., 2016):

- Accuracy (AC) is a review of how well the lesion image was segmented overall.

$$AC = \frac{TP+TN}{TP+TN+FP+FN} \quad (1)$$

- Jaccard index (JS) is a union over intersection of segmented lesions and ground truth masks (Powers, 2020).

$$JS = \frac{TP}{TP+FN+FP} \quad (2)$$

- Dice Coefficient (DC) is the similarity between the predicted results and the annotated ground truths.

$$DC = \frac{2 \times TP}{2 \times (TP+FN+FP)} \quad (3)$$

- Sensitivity (SE) shows the percentage of correctly identified skin lesion pixels.

$$SE = \frac{TP}{TP+FN} \quad (4)$$

- Specificity (SP) represents the percentage of pixels segmented as non skin lesions.

$$SP = \frac{TN}{TN+FP} \quad (5)$$

5.3 Comparative Experiments

5.3.1 Comparison on the ISIC 2016 Dataset

We trained and evaluated the suggested model using the ISIC 2016 dataset. The comparison of the suggested method with the state-of-the-art on the ISIC 2016 dataset is summarized in the Table 4. Different techniques have been used for segmentation. Yuan et al. (Yuan and Lo, 2017) achieved an AC value of 0.957 and a DC of 0.921. Also, Bi et al. (Bi et al., 2017) obtained an AC value of 0.953 and a DC of 0.921. Our method obtained promising results. We achieved an AC value of 0.9803 and a DC of 0.9433.

Figure 8 provides a visual representation of our suggested segmentation method of skin lesions. The experimental renderings can also be used to see how well the method works.

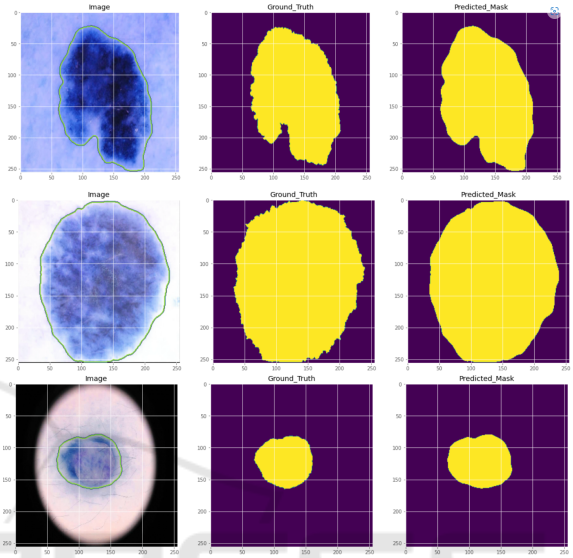

Figure 8: Segmentation results of our model on ISIC 2016 dataset.

5.3.2 Comparison on the ISIC 2017 Dataset

On the ISIC 2017 dataset, we further trained and tested the suggested network in this section. A comparison of the segmentation performance of the proposed network and other approaches is shown in Table 5. The metrics scores from the other models on this dataset are hardly sufficient because there are more images in this dataset that are difficult to segment precisely. Our suggested network still achieves satisfactory evaluation metrics. Attention-based DenseUNet showed that the segmentation of skin lesions was sufficiently successful to produce good results.

Figure 9 displays the results of the suggested model on this dataset of partially segmented skin lesion images. The outcomes also demonstrated how well our suggested network performed.

5.3.3 Comparison on the ISIC 2018 Dataset

We further evaluated the architecture using the ISIC 2018 dataset and compared our segmentations with the current state-of-the-art to determine how robust our suggested model was. The results are shown in

Table 4: Model performance on the ISIC 2016.

Approaches	AC	JS	DC	SE	SP
U-Net (Ronneberger et al., 2015)	0.936	0.782	0.868	0.930	0.935
FCN (Long et al., 2015)	0.941	0.813	0.886	0.917	0.949
Bi et al. (Bi et al., 2017)	0.953	0.859	0.921	0.962	0.945
Yuan et al. (Yuan and Lo, 2017)	0.957	0.849	0.913	0.924	0.965
Ours	**0.9803**	0.8564	**0.9433**	**0.9680**	**0.9855**

Table 5: Model performance on the ISIC 2017.

Approaches	AC	JS	DC	SE	SP
U-Net (Ronneberger et al., 2015)	0.913	0.687	0.781	0.825	0.976
SkinNet (Vesal et al., 2018)	0.932	0.767	0.851	0.930	0.905
MobileNetV3-UNet (Wibowo et al., 2021)	0.938	0.805	0.877	0.8624	0.963
Galdran et al. (Galdran et al., 2017)	0.948	0.767	0.846	0.865	0.980
Ours	**0.9619**	0.7160	0.8661	0.8490	**0.9892**

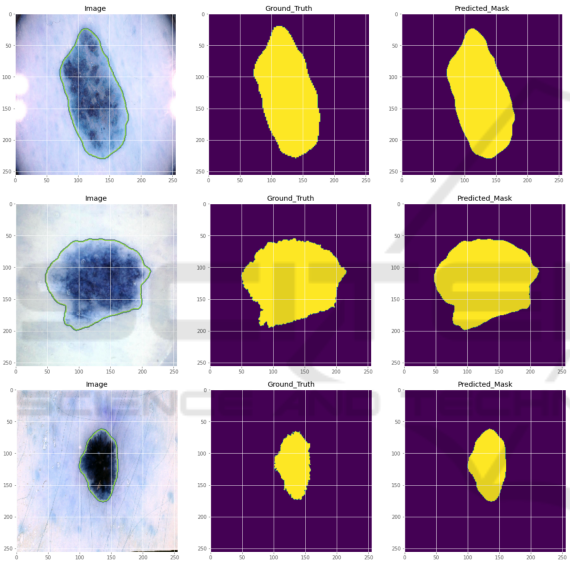

Figure 9: Segmentation results of our model in ISIC 2017 dataset.

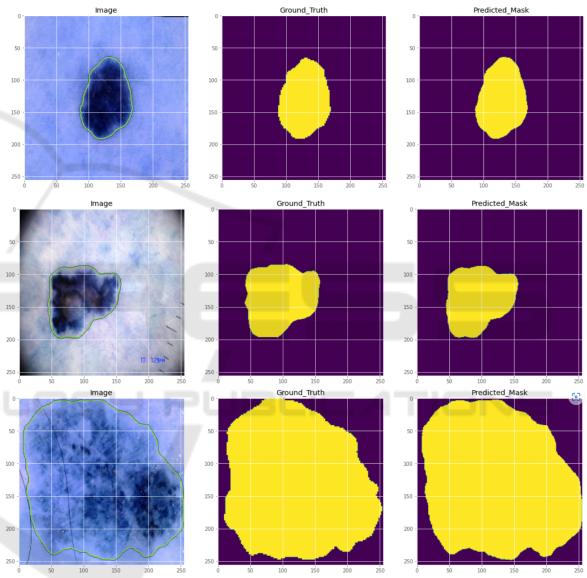

Figure 10: Segmentation results of our model in ISIC 2018 dataset.

Table 6 below. Our approach produced encouraging outcomes. We achieved an AC value of 0.9788 and a DC of 0.9228. Whereas, MobileNetV3-UNet (Wibowo et al., 2021) reached an AC of 0.9479 and DC of 0.9098. Another architecture, Unet++ (Zhou et al., 2019) obtained an AC of 0.952 and a DC of 0.872. According to the results, our model performed better than the current methods employed in the associative research area.

A visual representation of our suggested method for segmentation of skin lesions is shown in Figure 10. Experimental renderings can also be used to see how effective the algorithm is.

6 DISCUSSION AND PERSPECTIVES

There have been deep learning techniques based on DenseNet and U-Net used in medical images. The biggest challenges are the noise of images and the low contrast. Since U-Net has the ability to precise pixel-level localization, we suggested a model named DenseUNet based on DenseNet and U-Net. In the meantime, the attention mechanism (Arora et al., 2021) has been used in our module. The attention mechanism can enhance the precision of feature extraction by preventing missing pixel-level information. However, we improved the image contrast by

Table 6: Model performance on the ISIC 2018.

Approaches	AC	JS	DC	SE	SP
U-Net (Ronneberger et al., 2015)	0.890	0.549	0.647	0.708	0.964
R2U-Net (Alom et al., 2019)	0.880	0.581	0.679	0.792	0.928
Unet++ (Zhou et al., 2019)	0.952	0.796	0.872	0.89	0.970
MobileNetV3-UNet (Wibowo et al., 2021)	0.9479	0.8344	0.9098	0.9089	0.9638
Ours	**0.9788**	0.7990	**0.9228**	**0.9385**	**0.9897**

applying the adaptive gamma correction with weighting distribution.

Experimental results show that our model achieves state-of-the-art performance on three publicly available datasets due to the robustness of our model.

For future research, we will use Vision Transformers (ViT) for lesion segmentation. Also, we will create a software application to help the dermatologist segment the skin lesion for further diagnosis.

7 CONCLUSION

One of the hardest and most prevalent issues in image processing is image segmentation. Even human vision may not be accurate enough for this task, and in some situations, it may make a wrong or inaccurate diagnosis. Consequently, image segmentation is a challenging process. However, with the development of new approaches in recent years, considerable advancements in this field have been realized. In this paper, we successfully created a skin lesion segmentation method by combining CNN with a powerful algorithm that efficiently increases the contrast of the dermoscopic images. The combination of U-Net, DenseNet, and attention gate in our proposed method provides excellent results when compared to state-of-the-art.

REFERENCES

Alom, M. Z., Hasan, M., Yakopcic, C., Taha, T. M., and Asari, V. K. (2018). Recurrent residual convolutional neural network based on u-net (r2u-net) for medical image segmentation. *arXiv preprint arXiv:1802.06955*.

Alom, M. Z., Yakopcic, C., Hasan, M., Taha, T. M., and Asari, V. K. (2019). Recurrent residual u-net for medical image segmentation. *Journal of Medical Imaging*, 6(1):014006.

Arora, R., Raman, B., Nayyar, K., and Awasthi, R. (2021). Automated skin lesion segmentation using attention-based deep convolutional neural network. *Biomedical Signal Processing and Control*, 65:102358.

Baheti, B., Innani, S., Gajre, S., and Talbar, S. (2020). Eff-unet: A novel architecture for semantic segmentation in unstructured environment. In *Proceedings of the IEEE/CVF Conference on Computer Vision and Pattern Recognition Workshops*, pages 358–359.

Berseth, M. (2017). Isic 2017-skin lesion analysis towards melanoma detection. *arXiv preprint arXiv:1703.00523*.

Bi, L., Kim, J., Ahn, E., Kumar, A., Fulham, M., and Feng, D. (2017). Dermoscopic image segmentation via multistage fully convolutional networks. *IEEE Transactions on Biomedical Engineering*, 64(9):2065–2074.

Capdehourat, G., Corez, A., Bazzano, A., Alonso, R., and Musé, P. (2011). Toward a combined tool to assist dermatologists in melanoma detection from dermoscopic images of pigmented skin lesions. *Pattern Recognition Letters*, 32(16):2187–2196.

Codella, N., Rotemberg, V., Tschandl, P., Celebi, M. E., Dusza, S., Gutman, D., Helba, B., Kalloo, A., Liopyris, K., Marchetti, M., et al. (2019). Skin lesion analysis toward melanoma detection 2018: A challenge hosted by the international skin imaging collaboration (isic). *arXiv preprint arXiv:1902.03368*.

Codella, N. C., Gutman, D., Celebi, M. E., Helba, B., Marchetti, M. A., Dusza, S. W., Kalloo, A., Liopyris, K., Mishra, N., Kittler, H., et al. (2018). Skin lesion analysis toward melanoma detection: A challenge at the 2017 international symposium on biomedical imaging (isbi), hosted by the international skin imaging collaboration (isic). In *2018 IEEE 15th international symposium on biomedical imaging (ISBI 2018)*, pages 168–172. IEEE.

Galdran, A., Alvarez-Gila, A., Meyer, M. I., Saratxaga, C. L., Araújo, T., Garrote, E., Aresta, G., Costa, P., Mendonça, A. M., and Campilho, A. (2017). Data-driven color augmentation techniques for deep skin image analysis. *arXiv preprint arXiv:1703.03702*.

Gutman, D., Codella, N. C., Celebi, E., Helba, B., Marchetti, M., Mishra, N., and Halpern, A. (2016). Skin lesion analysis toward melanoma detection: A challenge at the international symposium on biomedical imaging (isbi) 2016, hosted by the international skin imaging collaboration (isic). *arXiv preprint arXiv:1605.01397*.

He, K., Zhang, X., Ren, S., and Sun, J. (2016). Deep residual learning for image recognition. In *Proceedings of the IEEE conference on computer vision and pattern recognition*, pages 770–778.

Hu, J., Shen, L., and Sun, G. (2018). Squeeze-and-excitation networks. In *Proceedings of the IEEE con-*

ference on computer vision and pattern recognition, pages 7132–7141.

Huang, G., Liu, Z., Van Der Maaten, L., and Weinberger, K. Q. (2017). Densely connected convolutional networks. In *Proceedings of the IEEE conference on computer vision and pattern recognition*, pages 4700–4708.

Huang, S.-C., Cheng, F.-C., and Chiu, Y.-S. (2012). Efficient contrast enhancement using adaptive gamma correction with weighting distribution. *IEEE transactions on image processing*, 22(3):1032–1041.

Kaul, C., Manandhar, S., and Pears, N. (2019). Focusnet: An attention-based fully convolutional network for medical image segmentation. In *2019 IEEE 16th international symposium on biomedical imaging (ISBI 2019)*, pages 455–458. IEEE.

Litjens, G., Kooi, T., Bejnordi, B. E., Setio, A. A. A., Ciompi, F., Ghafoorian, M., Van Der Laak, J. A., Van Ginneken, B., and Sánchez, C. I. (2017). A survey on deep learning in medical image analysis. *Medical image analysis*, 42:60–88.

Long, J., Shelhamer, E., and Darrell, T. (2015). Fully convolutional networks for semantic segmentation. In *Proceedings of the IEEE conference on computer vision and pattern recognition*, pages 3431–3440.

Mnih, V., Heess, N., Graves, A., et al. (2014). Recurrent models of visual attention. *Advances in neural information processing systems*, 27.

Nachbar, F., Stolz, W., Merkle, T., Cognetta, A. B., Vogt, T., Landthaler, M., Bilek, P., Braun-Falco, O., and Plewig, G. (1994). The abcd rule of dermatoscopy: high prospective value in the diagnosis of doubtful melanocytic skin lesions. *Journal of the American Academy of Dermatology*, 30(4):551–559.

Oktay, O., Schlemper, J., Folgoc, L. L., Lee, M., Heinrich, M., Misawa, K., Mori, K., McDonagh, S., Hammerla, N. Y., Kainz, B., et al. (2018). Attention u-net: Learning where to look for the pancreas. *arXiv preprint arXiv:1804.03999*.

Organization, W. H. et al. (2017). Radiation: Ultraviolet (uv) radiation and skin cancer. *Published October*, 16.

Pereira, S., Pinto, A., Alves, V., and Silva, C. A. (2016). Brain tumor segmentation using convolutional neural networks in mri images. *IEEE transactions on medical imaging*, 35(5):1240–1251.

Powers, D. M. (2020). Evaluation: from precision, recall and f-measure to roc, informedness, markedness and correlation. *arXiv preprint arXiv:2010.16061*.

Ronneberger, O., Fischer, P., and Brox, T. (2015). U-net: Convolutional networks for biomedical image segmentation. In *International Conference on Medical image computing and computer-assisted intervention*, pages 234–241. Springer.

Tschandl, P., Rosendahl, C., and Kittler, H. (2018). The ham10000 dataset, a large collection of multi-source dermatoscopic images of common pigmented skin lesions. *Scientific data*, 5(1):1–9.

Vesal, S., Ravikumar, N., and Maier, A. (2018). Skinnet: A deep learning framework for skin lesion segmentation. In *2018 IEEE Nuclear Science Symposium and Medical Imaging Conference Proceedings (NSS/MIC)*, pages 1–3. IEEE.

Wang, X., Girshick, R., Gupta, A., and He, K. (2018). Non-local neural networks. In *Proceedings of the IEEE conference on computer vision and pattern recognition*, pages 7794–7803.

Wibowo, A., Purnama, S. R., Wirawan, P. W., and Rasyidi, H. (2021). Lightweight encoder-decoder model for automatic skin lesion segmentation. *Informatics in Medicine Unlocked*, 25:100640.

Woo, S., Park, J., Lee, J.-Y., and Kweon, I. S. (2018). Cbam: Convolutional block attention module. In *Proceedings of the European conference on computer vision (ECCV)*, pages 3–19.

Xie, S., Girshick, R., Dollár, P., Tu, Z., and He, K. (2017). Aggregated residual transformations for deep neural networks. In *Proceedings of the IEEE conference on computer vision and pattern recognition*, pages 1492–1500.

Yuan, Y. and Lo, Y.-C. (2017). Improving dermoscopic image segmentation with enhanced convolutional-deconvolutional networks. *IEEE journal of biomedical and health informatics*, 23(2):519–526.

Zafar, K., Gilani, S. O., Waris, A., Ahmed, A., Jamil, M., Khan, M. N., and Sohail Kashif, A. (2020). Skin lesion segmentation from dermoscopic images using convolutional neural network. *Sensors*, 20(6):1601.

Zhou, Z., Siddiquee, M. M. R., Tajbakhsh, N., and Liang, J. (2019). Unet++: Redesigning skip connections to exploit multiscale features in image segmentation. *IEEE transactions on medical imaging*, 39(6):1856–1867.